

## Article

# A Field Study of Tropical Peat Fire Behaviour and Associated Carbon Emissions

Laura L. B. Graham <sup>1,2,\*</sup>, Grahame B. Applegate <sup>2</sup>, Andri Thomas <sup>1</sup>, Kevin C. Ryan <sup>3,†</sup>, Bambang H. Saharjo <sup>4</sup> and Mark A. Cochrane <sup>5</sup>

<sup>1</sup> Borneo Orangutan Survival Foundation, Bogor 16128, Indonesia; thomasandri@yahoo.com

<sup>2</sup> Tropical Forests and People Research Centre, University of the Sunshine Coast, Sippy Downs, QLD 4556, Australia; gapples@usc.edu.au

<sup>3</sup> US Forest Service, Missoula, MT 59808, USA; kryan.wildland.fire@gmail.com

<sup>4</sup> Faculty of Forestry and Environment, IPB University, Kampus IPB Darmaga, Bogor 16680, Indonesia; firebhsipb@apps.ipb.ac.id

<sup>5</sup> Appalachian Laboratory, University of Maryland Center for Environmental Science, Frostburg, MD 21613, USA; mark.cochrane@umces.edu

\* Correspondence: laura.graham@orangutan.or.id

† Retired.

**Abstract:** Tropical peatlands store vast volumes of carbon belowground. Human land uses have led to their degradation, reducing their carbon storage services. Clearing and drainage make peatlands susceptible to surface and belowground fires. Satellites do not readily detect smouldering peat fires, which release globally significant quantities of aerosols and climate-influencing gases. Despite national and international desire to improve management of these fires, few published results exist for in situ tropical peat fire behaviour and associated carbon emissions. We present new field methodology for calculating rates of fire spread within degraded peat (average spread rates, vertical  $0.8 \text{ cm h}^{-1}$ , horizontal  $2.7 \text{ cm h}^{-1}$ ) and associated peat volume losses ( $102 \text{ m}^3 \text{ ha}^{-1}$  in August,  $754 \text{ m}^3 \text{ ha}^{-1}$  in September) measured at six peat fire sites in Kalimantan, Indonesia, in 2015. Utilizing locally collected bulk density and emission factors, total August and September gas emissions of  $27.2 \text{ t ha}^{-1}$  ( $8.1 \text{ tC ha}^{-1}$ ) and  $200.7 \text{ t ha}^{-1}$  ( $60.2 \text{ tC ha}^{-1}$ ) were estimated. We provide much needed, but currently lacking, IPCC Tier 3-level data to improve GHG estimates from tropical peat fires. We demonstrate how calculations of total emission estimates can vary greatly in magnitude (+798% to −26%) depending on environmental conditions, season, peat burn depth methodology, bulk density and emission factors data sources, and assumed versus observed combustion factors. This illustrates the importance of in situ measurements and the need for more refined methods to improve accuracies of GHG estimates from tropical peat fires.

**Keywords:** climate change; greenhouse gases; haze; Indonesia; IPCC Tier 3; smouldering combustion



**Citation:** Graham, L.L.B.; Applegate, G.B.; Thomas, A.; Ryan, K.C.; Saharjo, B.H.; Cochrane, M.A. A Field Study of Tropical Peat Fire Behaviour and Associated Carbon Emissions. *Fire* **2022**, *5*, 62. <https://doi.org/10.3390/fire5030062>

Academic Editor: Alan F. Talhelm

Received: 17 March 2022

Accepted: 27 April 2022

Published: 29 April 2022

**Publisher's Note:** MDPI stays neutral with regard to jurisdictional claims in published maps and institutional affiliations.



**Copyright:** © 2022 by the authors. Licensee MDPI, Basel, Switzerland. This article is an open access article distributed under the terms and conditions of the Creative Commons Attribution (CC BY) license (<https://creativecommons.org/licenses/by/4.0/>).

## 1. Introduction

Although wildfires are episodic and variable as to both ecosystem and region in their severity, globally wildfire-derived atmospheric carbon emissions can make up greater than 50% of fossil fuel-based emissions [1–3]. In recent decades, emissions from fires in Indonesia's peatlands have become globally significant [4–7] and regionally deadly [8,9]. These emissions are wholly anthropogenic in nature due to human draining of these carbon rich wetlands but the severity of the fire problems are strongly tied to extreme drought conditions that allow surface fires to transition to smouldering fires within the underlying peat soils, which are themselves often closely associated with the intensity of El Niño events [10]. For these reasons, understanding fire behaviour in tropical peat is necessary for accurately estimating atmospheric carbon and other emissions from these peatlands when they do burn and, critically, gauging the potential effectiveness of planned mitigation activities to reduce them.

Fires in the drained peatlands of Indonesia's tropical peatlands cover ~200,000 km<sup>2</sup>, with peat dome profiles often exceeding 10 m depth at the centre, providing a globally critical reservoir of carbon of ~57 GtC [1]. Tropical peatlands, in their natural state, are forested, maintain year-round high water levels, and are naturally fire-resistant [2–5].

Logging, forest clearing, drainage, conversion to agriculture, and wildfire have rapidly degraded these ecosystems. In Indonesia, land-use changes brought about by increased human presence, have lowered water tables, dried near-surface peat soils, increased available surface fuels and expanded the use of fire [6–8]. By 2010, only 4% of the tropical peat swamp forest (TPSF) in Kalimantan and Sumatra was still identified as intact [9].

During 1997 and 2006, Indonesia had severe and prolonged dry seasons. In 1997, estimated fire-related peatland carbon emissions were 0.81–2.57 Gt, equivalent to 13–40% of the average annual global fossil fuel carbon emissions for that year [10]. Whilst in 2006, fires released an estimated  $49.15 \pm 26.81$  Mt of carbon from a 2.79 million ha study area in Central Kalimantan alone [11]. Global carbon emissions through fire, that are not balanced by regrowth, total  $0.5 \text{ Pg yr}^{-1}$ , of which  $0.1 \text{ Pg yr}^{-1}$  originates specifically from tropical peat burning [12].

The intense and prolonged dry season during the 2015 El Niño event resulted in extreme levels of peat burning and haze. Fire detections reached 831–915 per 1000 km<sup>2</sup> across Borneo and Sumatra [13]. Regional air quality and human health were severely compromised as these peatland fires released 3.2–11 Tg (PM<sub>2.5</sub>) of fine particulate matter [14] together with numerous other carcinogenic toxins from the partially combusted peat [15]. The city of Palangka Raya, on the island of Borneo, experienced months of unhealthy air quality, peaking in October 2015 when particulate matter levels reached  $3741 \mu\text{g m}^{-3}$  (PM<sub>10</sub>), more than ten times 'dangerous' PM levels [16]. Regionally, the toxic haze has been estimated to have resulted in over 100,000 deaths in 2015 [17,18]. The haze also impacted economic activity and the health of the populations in Singapore and Malaysia, substantially increasing political tensions between Indonesia and its neighbours [19,20]. Peat fire carbon emissions, in 2015, reached 11.3 Tg per day, exceeding emissions for the entire European Union during that period [21].

The majority of the haze and emissions come from slow, low temperature, smouldering peat fires which are difficult to detect from satellite, but which release vast volumes of noxious aerosols and climate-influencing gases [15,22]. Despite awareness of the impacts, national and international desire to stop them, and requirements to quantify associated emissions, very little data has been published describing in situ peat fire behaviour and related carbon emissions [23,24].

Peatland carbon emissions data have largely been estimated by proxy, using remotely sensed data from airborne LiDAR and optical satellites [11,25,26], as acknowledged by the IPCC (Intergovernmental Panel on Climate Change, 2013). Peat fire carbon emissions are estimated by multiplying the fire-affected area of peatland (not necessarily the actual area where fire burns down into the peat) by a series of parameters with varying degrees of accuracy, including average depth of peat burnt, peat bulk density, a combustion completeness factor, and emission factors for the major carbon species released by smouldering peat (mainly carbon dioxide, carbon monoxide and methane) [15,24,26,27]. Satellite sensors, such as Landsat and MODIS, can be used to remotely assess the extents of surface area burned. However, clouds, smoke, overpass times, spectral limitations and spatial resolutions of the observations present challenges for providing timely information and accurate classifications [28–30]. Regardless, these techniques only show areas of peatland subjected to surface fires, not whether peat fires occurred or their depth of burning [31].

Peat fire depth of burn can be estimated using LiDAR data. However, this requires collection of aerial data before and after. It is costly and logistically difficult to collect such data. Consequently, this has been rarely conducted and at limited locations [11,25,26], making extrapolations or estimations of burn depths to other locations and fire years necessary. Surface fuel loads, bulk density and carbon content of the peat vary across the landscape and can only be quantified through direct measurement [12]. These elements

remain largely understudied [21,23,26,32,33] and are thus crudely estimated with average values for entire landscapes [31]. Similarly, the ways in which fire moves through the peat and the variability of depth burned, in relation to other environmental features, remains poorly understood [32]. Estimates are largely derived from lab-based, temperate peat studies [34–37].

Peat fires initiate and spread at lower temperatures and under lower oxygen levels than flaming surface fires, despite high peat moisture contents [38]. Smouldering peat fires travel extremely slowly, with observed spread rates in temperate environments as low as 0.5 m per week [39] over long periods (weeks–months) despite rain and weather changes. Smouldering fires result in incomplete combustion and emit dangerously high levels of noxious chemicals [15,38,40].

To investigate tropical peat fire behaviour and related emissions, methods for detailed measurement of the rate of tropical peat fire spread and peat volume loss were developed and carried out in the field [41]. We applied these findings, together with bulk density [42] and GHG emission factors specific to this region [15] to derive estimated GHG emissions, as per the IPCC emissions from organic soil fire equation (IPCC, 2013). Here, we present the first tropical peatland GHG emissions estimates using parameters based completely on data collected in situ from actively burning peat fires and compare these findings with results from previous studies to explore methodological and assumption-based limitations or uncertainties.

## 2. Materials and Methods

Originally covered by continuous tropical peat swamp forest, the ‘Mawas’ peat dome (>310,000 ha) is situated between the Kapuas and Barito rivers in Central Kalimantan, Indonesia. Annual rainfall averages approximately 3000 mm at the site, with typical dry seasons from July to November (Figure 1a). Interannual variation impacts wet and dry season intensity, with 2015 being a drier than average year (Figure 1b). Since the 1980s, the area has become increasingly degraded due to logging (legal and illegal) [43], drainage, land clearing and uncontrolled fires, most notably during 1997–1998, after inclusion in the Indonesian Government’s Mega Rice Project (MRP) [44]. The MRP aimed to convert one million ha of tropical peatland to rice production. More than 4000 km of canals were dug and large areas of forest were cleared across lowland Central Kalimantan [44]. However, natural tropical peatland is a poor medium for growing rice. Rice production failed and many drained peatlands burned during the severe 1997–98 El Niño dry season [8,10,44].

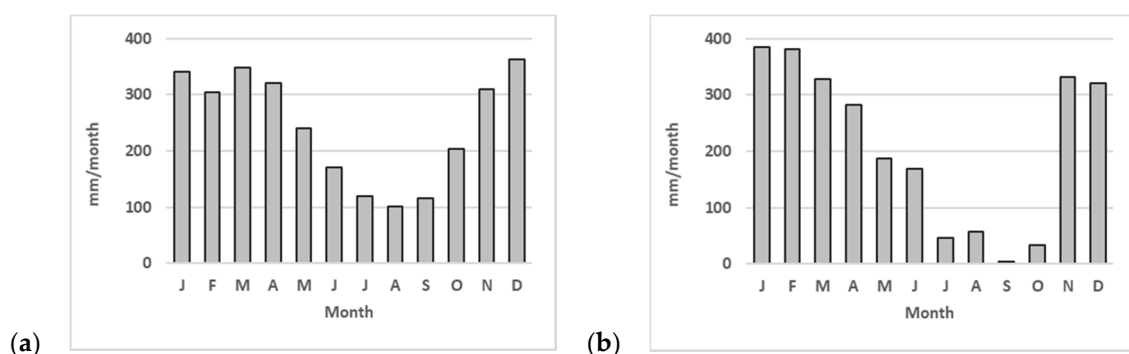


**Figure 1.** Precipitation patterns for the Mawas study region in Central Kalimantan, Indonesia. (a) Average monthly precipitation, 1983–2020. (b) Average monthly precipitation, 2015 (data source Global Precipitation Climatology Project (GPCP) and Global Precipitation Measurement (GPM)).

This largely hemic peat dome is classified by the Indonesian Government as a mix of protected forest, conservation area and some small ‘areas for other use’. Northern sections remain forested and, to a greater degree, intact. Across southern sections of the dome, the extensive canal network has led to continuously low water tables. Near-annual surface fires, that often transition to smouldering peat fires, have resulted in near-complete loss

of the original forest cover, leaving the area dominated by ferns and sedges and sporadic pioneer tree individuals.

This analysis focuses on results from studies within ~50,000 ha in the south-west section of the dome (Figure 2). The total study site burn area for the month of August and September 2015 was calculated based on VIIRS hotspots data, downloaded from NASA's Fire Information for Resource Management System (FIRMS), and restricted to the focal study area and respective months, followed by analysis of the burn area [45]. A concave hull (alpha shapes, threshold hull of 0.05) algorithm was used to draw a boundary around the observed hotspots, to give an approximation of the area burned specific and restricted to these two months (Figure 2b).

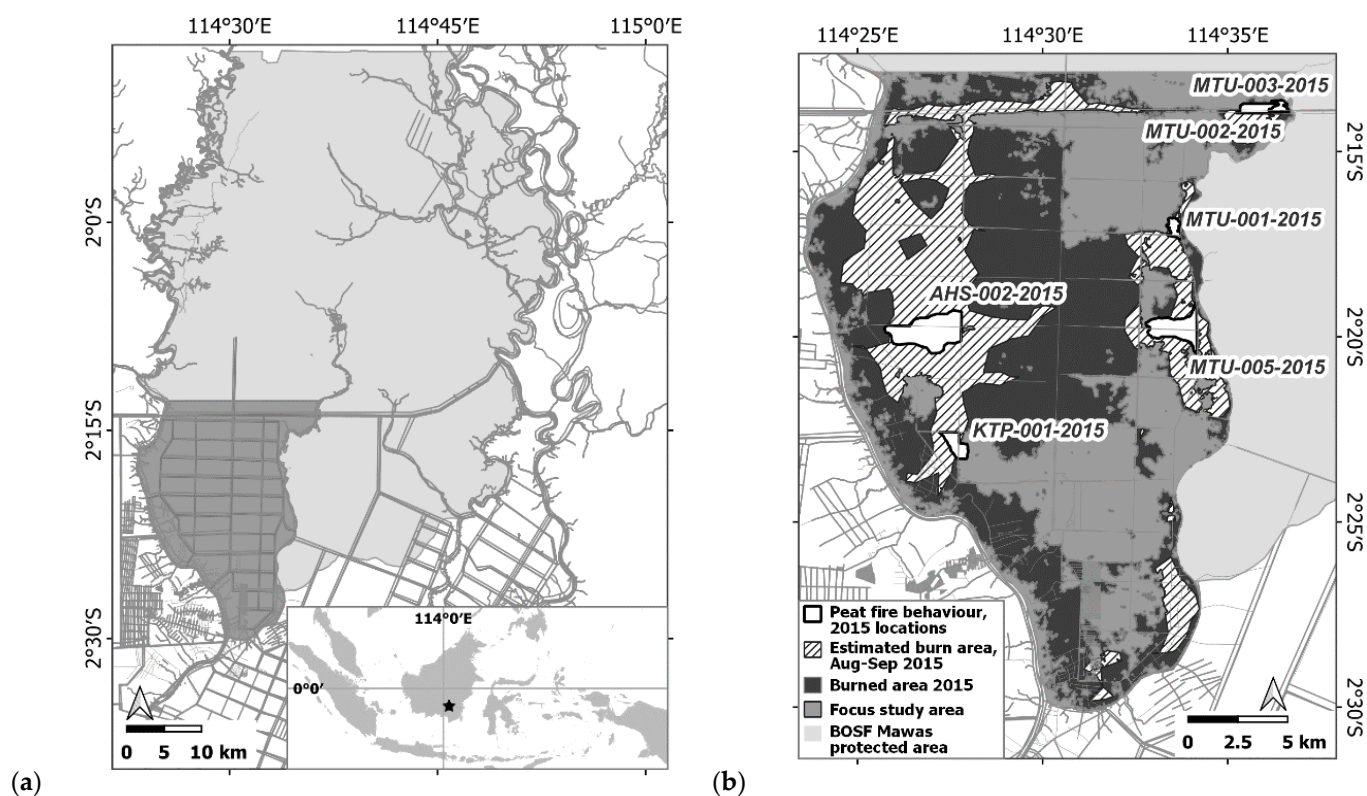


**Figure 2.** Study region: (a) the entire Mawas peat dome (light shading), with the area where fires were analysed highlighted in darker shading. Straight lines are drainage canals and meandering features are natural rivers and streams. Inset shows position of site within Indonesia. (b) Focus study area (approx. 50,000 ha), showing the extent of burnt area throughout 2015 (black [45]), specific to the months of August–September 2015 (striped), and the areas of the six peat fires presented in this study.

Fires were detected by satellite (<http://modis-catalog.lapan.go.id/monitoring/hotspot/index>, accessed daily during September and October 2015) or reported through community networks. The Fire Scene Evaluation (FSE) and peat fire behaviour methods [41] utilize a standardized 67-question and measurement form. The two-part FSE form facilitates detailed and consistent collection and recording of wide-ranging environmental factors and biophysical aspects of fires. Part I records weather (relative humidity, wind and temperature), area burned (calculated through marking the perimeter with a hand-held GPS), distance from nearest water source, number of times previously burned, etc. Part II, conducted only if the underlying peat has ignited, focuses on measuring peat-fire behaviour, including rate of peat-fire spread, volume of peat burned, peat moisture content and water table depth, as well as social and fuel aspects of peat fires [46]. Fire locations are often remote, so even after locations are reported by local residents or detected in satellite imagery, conducting a single FSE takes the research team up to three days, plus two-day return travel to the site. Additionally, peat samples must be processed in a lab, requiring



an additional week. Given conditions conducive to peat fires usually occur for no more than two months a year, there are practical limits to the amount of data which can be collected. Site-specific peat bulk density and emission factor values are sourced from two previous studies [15,42]. The data presented here were collected during the 2015 dry season (July–November).

### 2.1. Rate of Peat Fire Spread

At the edge of smouldering peat fires, metal rods with unique identifiers (in sets of 4–7, depending on width of the active peat fire), 8 mm in diameter and 1.3 m in length, were inserted into burning peat faces. Rods had lines etched 70 cm from one end and were inserted until the etch point was at the height of the peat surface, with rods for each set inserted approximately 40 cm apart. Where possible, this layout was repeated at several positions around the burning perimeter of the peat fires. After approximately 24 h (with the exact time interval recorded), depth of burn at each rod and horizontal distance and direction (compass bearing) to nearest and farthest points on the peat-burn interface from each rod were measured (within a finite rectangular area in the direction of fires spread, with the width defined by the iron rods' mid-point distance) (Figures 3a and 4a). Because the peat did not burn in uniform patterns, measuring nearest and farthest burning distances from rods provided a measure of heterogeneity.

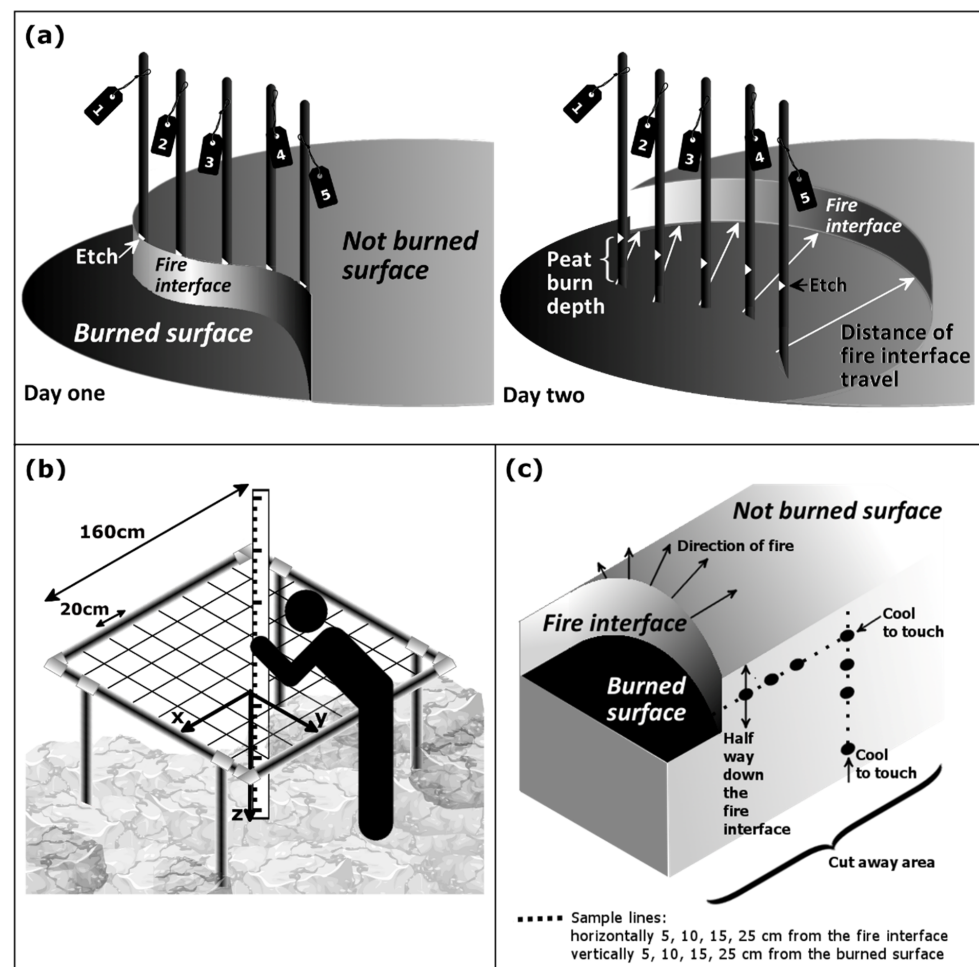


**Figure 3.** Diagrams showing methods for (a) recording peat fire spread rates, (b) peat volume loss measurements and (c) peat core sampling for moisture content analysis.



**Figure 4.** Photos of methods for (a) recording peat fire spread rates, (b) peat volume loss measurements and (c) peat core sampling for moisture content analysis.

Rates of spread were estimated by first calculating the average spread distance for each respective rod, based on its nearest and farthest measurements. For each rod set, data from all rods were averaged to estimate both horizontal and vertical hourly rates of spread. Rod set averages were treated as replicate samples.

## 2.2. Volume of Peat Consumed through Burning

Before and after fire, peat surfaces were mapped using a 160 cm sampling square, with a  $20 \times 20$  cm mesh grid, providing a repeatable matrix of 81 intercept points. The square was levelled, 1 m above the nominal peat surface. Four metal rods were inserted into the peat adjacent to each grid corner to mark exact locations. Each rod was etch marked at the pre-fire peat surface. Grids were set up just ahead of peat-fire interfaces in the direction of prevalent fire movement. At each intercept point, a measuring pole, orthogonal to the sampling matrix, was used to measure distance (z) to the unburnt peat surface, providing x, y, z peat surface measurements (Figures 3b and 4b). This was conducted at one or two positions ahead of peat-fire interfaces at each FSE location. Several days later, after fire had passed through the mapped locations and stopped burning vertically down into the peat, sampling squares were re-established at the precise locations, orientation and height, using the metal rods that had been left in place with the original peat surface etch marks. All x, y, z points were re-measured for the post-fire peat surface.

Peat volume loss was calculated from differences between the x, y, z coordinates collected before and after the fire [41]. To calculate the change in volume, the area under the grid was subdivided into abutting prisms, where each prism's base had the dimensions of the grid, i.e.,  $20 \times 20$  cm (Figure 5a,b). Volume under the grid was estimated to be a sum of 'prisms' obtained by linear interpolation between the four heights given at the corners of each grid square (Figure 5c). The ground surface of each prism does not need to be level (Figure 5d). To account for uneven surfaces, the volume of each grid, or each of

the square-based prisms, was subdivided into two ‘truncated right triangular prisms’ for subsequent evaluation (Figure 5e).

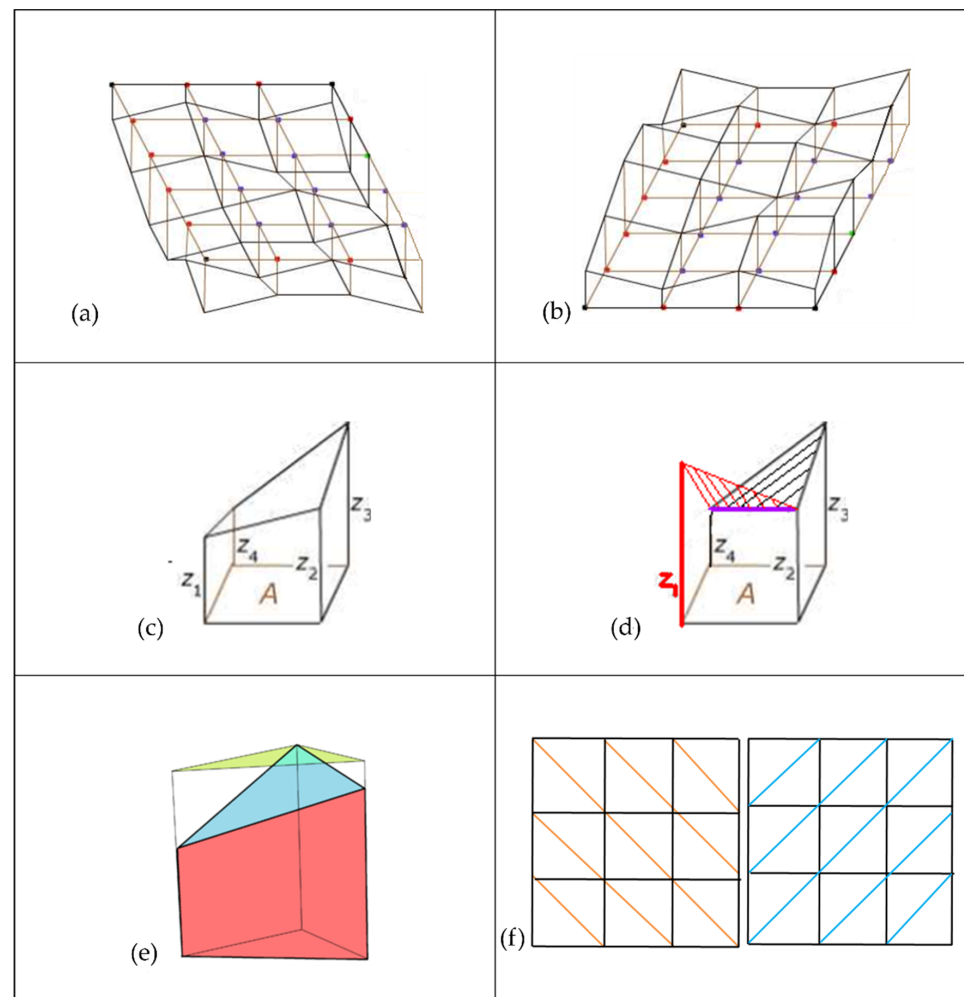


**Figure 5.** Measuring peat volume loss: (a) illustration of volume between the sampling grid (uppermost) and peat surface, (b) diagram in (a) flipped vertically—peat surface now uppermost (c) illustrated grid square volume calculations of a single prism by linear interpolation between the four corner heights when the peat surface is flat and (d) irregular, (e) volume of a truncated right triangular prism, (f) subdividing the square-based prisms from left to right, creating left-to-right triangular prisms, and then right-to-left-to triangular prisms. Illustrations (a–d) from (and modified from) [47].

Given the irregular surface of the peat, the volume calculation was further improved by dividing each square-based grid prism diagonally from left to right and then again from right to left, taking the average of the two volume calculations (Figure 5f). Thus, using the original prism labels (Figure 5c), the volume of each square-based prism is:

$$V = 1/4 * A * (z_1 + z_2 + z_3 + z_4) \quad (1)$$

where  $A$  is the area of the base and  $z_1, z_2, z_3, z_4$  are heights at the four corners [47].

When volumes of all prisms are summed, each corner height ( $z_1$ – $z_4$ ) will occur once for each prism that its edge abuts, so 1, 2, 3, or 4 times according to the position of its base point in the grid. Thus, the volume under the grid is:

$$1/4 * A * (\sum h_1 + 2\sum h_2 + 3\sum h_3 + 4\sum h_4) \quad (2)$$

where  $A$  is the area of a grid rectangle and  $h_1$ ,  $h_2$ ,  $h_3$  and  $h_4$  are measurements at each grid intersection.

It is noteworthy that the peat volume method also provided an alternative to using the iron rods for estimating depth of peat burnt. Furthermore, on a micro-scale, it quantifies burnt and unburnt area, thus, providing the area that has actually experienced peat fire. The actual combustion factor for the observed area can be quantified instead of assuming it to be 1 (complete), as generally occurs in the literature.

### 2.3. Peat Moisture Content

At the peat fire interface, an approximate  $50 \times 50$  cm section of peat was dug away, perpendicular to the interface. Half-way down, and parallel to the fire interface, a 2.5 cm diameter soil corer was used to extract peat samples (approx. 80 g each) from the excavated wall. Samples were taken at 5, 10, 15 and 25 cm, horizontally, and then, additionally, every 10 cm away from the interface, until the peat was ‘cool to touch’. Additional samples were similarly taken at 5 cm intervals (e.g., 5, 10, 15, 25 cm) vertically down into the peat until it felt cool (Figures 3c and 4c). Three replicate samples were taken for each position. These peat samples were sealed in small plastic sample bags. In the laboratory, samples were weighed, dried to a constant weight, then weighed again. Percentage moisture content was calculated as  $(\text{wet weight} - \text{dry weight}) \times 100 / \text{wet weight}$  of the peat sample, with averages calculated across replicates for each position.

### 2.4. Water Table Depth

Two dipwells (PVC pipes, 4.5 cm in diameter, 4 m long, with 0.5 cm diameter holes drilled at 7 cm intervals along the length of the pipes) were inserted 3.7 m into the peat, 10 m behind and 10 m in front of the peat-fire interface. Water levels were left to stabilize for 24 h, then water table depths of each dipwell were measured using the blow-straw method [48].

## 3. Results

During the August to September study period of the 2015 dry season, approximately 10,000 ha of the 50,000 ha focal study area burned. Of the ten investigated fire scene evaluations (FSEs) conducted during this period, six had transitioned from the surface, and become the peat fires described in this study. The six peat-fire FSEs covered approximately 1000 ha, 10% of the burned area. Of these 10 FSEs, only 6 included burning peat, and these are the FSEs presented below. Three of these peat fires were evaluated for rate of peat-fire spread, five for peat volume loss and four for moisture content. There were two peat fires at which all investigated aspects of peat-fire behaviour were collected.

### 3.1. General Environmental Conditions

At each FSE location, the environmental data collected included ambient air temperature, relative humidity and wind speed, water table depth (WTD), both ahead and behind the peat-fire interface, and distance to nearest surface water source (usually a canal). Additionally, fire frequency or history (i.e., how many previous fires had occurred at that location [45]) and surface area burned were recorded. Fires that occurred on raised peat berms along canal banks, where excavators deposited the dug-out peat, were also noted.

The FSEs included peat fires that occurred during August and September 2015. Temperature and relative humidity ranged from  $32.0$ – $36.6$  °C and 37–52%, respectively. Wind speeds were  $0.4$ – $2.1$  m s<sup>−1</sup>. WTD varied widely, from 36–136.5 cm, with the wide range affected by proximity of fires to both canals and berms, which disrupts water table depths, and depths from peat surface to the water table, respectively. Most fires began near canals (0–20 m) with only two occurring further inland (50 m and 130 m). No peat fires further from canal banks were observed although we cannot rule out occurrence at such locations beyond the field of view. Two fires ran along the raised berms. All FSE locations had



burned previously, between three to eight times from 1990–2009. Fire sizes ranged from 34–500 ha (see FSE field sketches and photos—Supplementary Material S1).

### 3.2. Moisture Content and Bulk Density

In addition to environmental data recorded directly at the field site, peat samples were taken ahead of the peat-fire interface and returned to the laboratory to estimate peat moisture content. Fuel moisture contents ranged from 59–87% horizontally and 80–88% vertically, at the points where peat became cool to touch, i.e., the state of peat before being heated by the advancing fire. Average peat bulk density of the top 40 cm, used for all FSE locations, was  $0.1428 \pm 0.0218 \text{ g cm}^{-3}$ , derived from previous sampling and analysis at the site [42].

### 3.3. Rate of Peat Fire Spread

Horizontal and vertical rates of peat fire spread over ~24 h were investigated at multiple points along fire perimeters ( $n = 1\text{--}6$ —dependent upon available extent of peat fire at which metal rod measurement sets could be installed) at three separate fire sites (Table 1), with average (and standard deviation) vertical and horizontal spread rates calculated. Vertical spread rates averaged  $0.8 \pm 0.3 \text{ cm h}^{-1}$ , while average horizontal spread rates were  $2.7 \pm 1.6 \text{ cm h}^{-1}$ . However, vertical and horizontal spread rates for two peat fires were very similar (~1.0 and ~3.65  $\text{cm h}^{-1}$ ), while the other peat fire had much lower vertical (~40%) and horizontal spread rates (~27%). Among individual rods, spread rates varied widely with maximum observed vertical and horizontal spreads of 2.3 and 9.3  $\text{cm h}^{-1}$ , respectively, and corresponding minimum rates of 0.2 and 0.3  $\text{cm h}^{-1}$ .

**Table 1.** Vertical and horizontal rate of peat fire spread for three fire scene evaluation sites, shown as average rates (with standard deviation) of spread for all points of observation. Rod sets include 6 individual rod locations.

| FSE Code        | Vertical Burn Depth ( $\text{cm h}^{-1}$ ) |      |      | Horizontal Burn Spread ( $\text{cm h}^{-1}$ ) |      |      | <i>n</i> (Number of Rod Sets) |
|-----------------|--|------|------|---|------|------|-------------------------------|
|                 | Ave.                                       | Max. | Min. | Ave.  | Max. | Min. |                               |
| MTU-002         | $0.9 \pm 0.5$                              | 2.3  | 0.2  | $3.6 \pm 1.9$                                 | 9.3  | 0.3  | 6                             |
| AHS-002         | $0.4 \pm 0.2$                              | 1.0  | 0.2  | $0.9 \pm 0.4$                                 | 2.2  | 0.4  | 2                             |
| MTU-005         | $1.1 \pm 0.2$                              | 1.5  | 0.9  | $3.7 \pm 2.5$                                 | 8.2  | 1.1  | 1                             |
| Overall average | $0.8 \pm 0.3$                              | 2.3  | 0.2  | $2.7 \pm 1.6$                                 | 9.3  | 0.3  |                               |

### 3.4. Peat Volume Loss through Burning

Nine peat volume loss sampling grid sites were established across five separate fire locations (with  $n$  representing the number of grids per FSE location, Table 2). Peat volume losses ranged from 50 to 804  $\text{m}^3 \text{ ha}^{-1}$  per location, averaging  $493 \pm 361 \text{ m}^3 \text{ ha}^{-1}$ . When stratified by month, August 2015 peat volume losses averaged  $102 \pm 74 \text{ m}^3 \text{ ha}^{-1}$ , whereas during September, when lower water tables existed across the peat dome, average peat volume losses increased to  $754 \pm 50 \text{ m}^3 \text{ ha}^{-1}$  (Table 2).

Observed peat burn depths at the five FSE locations ranged from 0–30 cm for all measures, with average depths at individual locations from 0.7 cm to 8.5 cm. The overall average of all locations was  $5.0 \pm 3.6 \text{ cm}$ . It was uncommon for an observed gridded surface area to burn completely. Surface area coverage of locations experiencing peat fire ranged from 14–96% (average 75%) based on numbers of grid cells actually burned. When limited to grid cells that actually burned, average burn depth was  $6.3 \pm 3.6 \text{ cm}$ . Depth of burn differed substantially between months, averaging 1.2 cm in August and 7.5 cm in September. Similarly, average percentage of peat fire area burned increased from 54% to 89%, respectively.

Dividing the observed average monthly peat volume losses (which include burned and unburned grids) by similarly calculated monthly averages derived solely from burned grid cells ( $237 \pm 103 \text{ m}^3 \text{ ha}^{-1}$  for August and  $852 \pm 88 \text{ m}^3 \text{ ha}^{-1}$  for September) yields fractions corresponding to volumetric monthly combustion factors of 43% and 88% in August and September, respectively.

**Table 2.** Peat volume losses and peat burn depths observed using the matrices method. Burn depths are averages of all grid depth changes within matrices, including zero change, then excluding unburned grids (burned only), with area of grid burned (%) and the number of matrices (*n*) per fire scene evaluation shown. Each of the matrices had 81 sample points.

| FSE Code        | Date of Initial FSE | Peat Volume Loss ( $\text{m}^3 \text{ ha}^{-1}$ ) | Depth of Burn from Volume Grids (cm) |       |                    | Area of Grid Burned (Avg.) (%) | <i>n</i> |
|-----------------|---------------------|---|--------------------------------------|-------|--------------------|--------------------------------|----------|
|                 |                     | Avg.  | All Grids (Avg.)                     | Max.* | Burned Only (Avg.) |                                |          |
| MTU-001         | 20/08/15            | $50 \pm 47$                                       | $0.7 \pm 0.6$                        | 11.3  | $4.2 \pm 1.3$      | $14 \pm 0.1\%$                 | 2        |
| MTU-003         | 23/08/15            | $154 \pm 0$                                       | $1.6 \pm 0$                          | 11.2  | $1.7 \pm 0$        | $94 \pm 0\%$                   | 1        |
| KTP-001         | 09/09/15            | $754 \pm 90$                                      | $7.3 \pm 0.8$                        | 27.4  | $7.6 \pm 0.3$      | $96 \pm 0.1\%$                 | 2        |
| AHS-002         | 06/09/15            | $704 \pm 407$                                     | $6.8 \pm 4.0$                        | 26.6  | $7.9 \pm 4.4$      | $85 \pm 0.0\%$                 | 2        |
| MTU-005         | 15/09/15            | $804 \pm 78$                                      | $8.5 \pm 0.5$                        | 30.0  | $10.2 \pm 1.9$     | $86 \pm 0.2\%$                 | 2        |
| Aug Average     |                     | $102 \pm 74$                                      | $1.2 \pm 0.6$                        | 11.3  | $3.0 \pm 1.8$      | $54 \pm 0.6\%$                 |          |
| Sept Average    |                     | $754 \pm 50$                                      | $7.5 \pm 0.9$                        | 28.0  | $8.6 \pm 1.4$      | $89 \pm 0.1\%$                 |          |
| Overall Average |                     | $493 \pm 361$                                     | $5.0 \pm 3.2$                        | 21.3  | $6.3 \pm 3.0$      | $75 \pm 34\%$                  |          |

\* Minimum burn depth for all grids was 0 cm.

### 3.5. Calculating Carbon Emissions

Established methods [24] for calculating total peat carbon emissions involve multiplying the area and depth of peat burnt by peat bulk density, a combustion completeness factor and emission factors:

$$E = A \times D \times BD \times CF \times EF \times 10^{-3} \quad (3)$$

where *E* represents total gas emissions ( $\text{t ha}^{-1}$ ), *A* is area burned (ha), *D* is average burn depth (m), *BD* is average bulk density ( $\text{g cm}^{-3}$ ), *CF* is the combustion completeness factor (usually taken to be 1 and dimensionless), and *EF* are emission factors for each gas ( $\text{g kg}^{-1}$ ). Emission factors for the region (Stockwell et al. 2016) used in this study are the three major carbon trace gases: carbon dioxide ( $1564 \pm 77 \text{ g kg}^{-1}$ ), carbon monoxide ( $291 \pm 49 \text{ g kg}^{-1}$ ) and methane ( $9.51 \pm 4.74 \text{ g kg}^{-1}$ ); ‘*E*’ (the amount of gas emissions) can also be evaluated to present the carbon contents of the three gases (carbon-tonnes  $\text{ha}^{-1}$ ).

In the IPCC equation,  $A \times D$  is the burned volume of peat. We directly measured consumed volumes, using the truncated triangular prism summation formulae per grid, as described above. We can then apply, either the peat volume lost result calculated by using the all grids burned and apply combustion factor of 1, or use peat volume lost results calculated by using the burned only grids and our calculated combustion volume percentages as our combustion factor (43% and 88% for August and September, respectively)—which gives the same emission result (although SD differs due to the different elements in the formula), i.e., we have actual 100% combustion completeness rather than assumed. We used these data to calculate combined gas emissions for the three major trace gases during the 2015 dry season. Using the combustion factor volume percentage, August estimates for total gas emissions were  $27.2 \pm 26.1 \text{ t ha}^{-1}$ , or  $8.1 \pm 7.8 \text{ tC ha}^{-1}$ , whereas September total emissions increased to  $200.7 \pm 45.6 \text{ t ha}^{-1}$ , or  $60.2 \pm 13.7 \text{ tC ha}^{-1}$  (Table 3). Using published IPCC emission factors [24] would yield total emission estimates that are ~4% higher and total carbon emissions approximately ~2% higher in both months.

**Table 3.** Total gas and carbon emissions per hectare from peat burning in Central Kalimantan during August and September 2015, based on the IPCC formula, using parameters from field data. The emissions are calculated using both burned and non-burned grids combined, i.e., with CF of 1, and where CF% is specifically calculated based on burned only grid volume in the matrix (shaded cells, emissions unaltered).

| Total Emissions    |                    | Total Carbon Emission |      | Burn Volume                     |     | Bulk Density       |        | Combustion Factor |      | Emission Factor (Total Gas Weight) ** |         | Carbon Emission Factors by Gas |                     |         |        |
|--------------------|--------------------|-----------------------|------|---------------------------------|-----|--------------------|--------|-------------------|------|---------------------------------------|---------|--------------------------------|---------------------|---------|--------|
| Formula Components |                    | E                     |      | A × D                           |     | BD                 |        | CF                |      |                                       |         | EF                             |                     |         |        |
| Units              | t ha <sup>-1</sup> | C-t ha <sup>-1</sup>  |      | m <sup>3</sup> ha <sup>-1</sup> |     | g cm <sup>-3</sup> |        | Dimensionless     |      | g kg <sup>-1</sup>                    |         | Carbon Weight % *              | gC kg <sup>-1</sup> |         |        |
| August 2015        | ±                  |                       | ±    | average                         | ±   | average            | ±      |                   | ±    | average                               | ±       |                                | average             | ±       |        |
| Total (CF = 1)     | 27.2               | 20.2                  | 8.1  | 6.0                             | 102 | 74                 | 0.1428 | 0.0218            | 1    | 1864.51                               | 91.39   | 0.300                          | 558.735             | 29.928  |        |
| Total (CF = %)     | 27.2               | 26.1                  | 8.1  | 7.8                             | 237 | 103                | 0.1428 | 0.0218            | 0.43 | 0.71                                  | 1864.51 | 91.39                          | 0.300               | 558.735 | 29.928 |
| Carbon dioxide     | 22.8               | 21.9                  | 6.2  | 6.0                             | 237 | 103                | 0.1428 | 0.0218            | 0.43 | 0.71                                  | 1564.00 | 77.00                          | 0.273               | 426.834 | 21.014 |
| Carbon monoxide    | 4.2                | 4.1                   | 1.8  | 1.8                             | 237 | 103                | 0.1428 | 0.0218            | 0.43 | 0.71                                  | 291.00  | 49.00                          | 0.429               | 124.781 | 21.011 |
| Methane            | 0.1                | 0.1                   | 0.1  | 0.1                             | 237 | 103                | 0.1428 | 0.0218            | 0.43 | 0.71                                  | 9.51    | 4.74                           | 0.749               | 7.120   | 3.549  |
| September 2015     | ±                  |                       | ±    | average                         | ±   | average            | ±      |                   |      | average                               | ±       |                                |                     |         |        |
| Total (CF = 1)     | 200.7              | 34.8                  | 60.2 | 10.5                            | 754 | 50                 | 0.1428 | 0.0218            | 1    | 1864.51                               | 91.39   | 0.300                          | 558.735             | 29.928  |        |
| Total (CF = %)     | 200.7              | 45.6                  | 60.2 | 13.7                            | 852 | 88                 | 0.1428 | 0.0218            | 0.88 | 0.02                                  | 1864.51 | 91.39                          | 0.300               | 558.735 | 29.928 |
| Carbon dioxide     | 168.4              | 38.2                  | 46.0 | 10.4                            | 852 | 88                 | 0.1428 | 0.0218            | 0.88 | 0.02                                  | 1564.00 | 77.00                          | 0.273               | 426.834 | 21.014 |
| Carbon monoxide    | 31.3               | 8.7                   | 13.4 | 3.7                             | 852 | 88                 | 0.1428 | 0.0218            | 0.88 | 0.02                                  | 291.00  | 49.00                          | 0.429               | 124.781 | 21.011 |
| Methane            | 1.0                | 0.6                   | 0.8  | 0.4                             | 852 | 88                 | 0.1428 | 0.0218            | 0.88 | 0.02                                  | 9.51    | 4.74                           | 0.749               | 7.120   | 3.549  |

\* (<https://www.webqc.org/mmcalc.php>) (accessed on 7 September 2019); \*\* Stockwell et al. 2016.

## 4. Discussion

The objective of this study was to collect in situ data on burning tropical peat, relate it to prevailing environmental conditions, and apply empirically derived parameters to calculate estimated carbon emissions. Despite all sampling being conducted within a single peat dome, substantial variability was evident within and between peat fires. Here we discuss how environmental conditions and methodologies used might explain this variability and place these findings in the context of previously published studies. The goal is to enable consistent and accurate use and interpretation of data, collected both in situ and remotely by fostering improved understanding of peat fire behaviour in these systems.

### 4.1. Rate of Peat Fire Spread and Current Environmental Factors

Rates of peat fire spread do not directly enter into peat-fire total carbon emissions calculations. However, they help us to understand how environmental factors influence tropical peat-fire behaviour and affect subsequent areas and depths of burn.

In a degraded Kalimantan hemic peatland, which has experienced numerous previous fires, observed peat fires averaged horizontal spread rates of  $2.7 \text{ cm h}^{-1}$ , and vertical downward rates of  $0.8 \text{ cm h}^{-1}$ . High standard deviations both within individual peat fires (observed using multiple iron rod sets) and between individual peat fires illustrate this characteristic variability. Maximum horizontal and vertical spread rates were  $9.3$  and  $2.3 \text{ cm h}^{-1}$ , respectively, with corresponding minimum rates of  $0.3$  and  $0.2 \text{ cm h}^{-1}$ .

Most observed peat fires self-extinguished within 24–48 h, and nearly all before 72 h after initial observation. In temperate and boreal systems, continued burning of peat fires has been observed for weeks, if not months, and tropical peat fires have been assumed to do the same, given continued surface fire detections and extreme haze levels. However, our extensive field observations across degraded peatlands that have previously burned many times, suggest that peat fires can regularly develop from surface fires and move through the peat for relatively short periods before expiring, whilst intermittently igniting new surface fires that subsequently lead to numerous additional peat fires developing. The process results in a complex landscape that is pockmarked with areas with and without peat consumption, versus uniform amounts of peat consumption across a burned area, such as may have occurred shortly after drainage. It is noteworthy that the studied peat dome has been degraded by many previous fires over the last 25 years and now has low surface fuel loads and increasingly compacted peat. Peat bio-physical structure, and, presumably, peat-fire behaviour, is likely to differ from when the system first became degraded, when peat structure and greater amounts of surface fuels will have likely encouraged greater numbers of peat ignitions and depths of peat fires [49].

### 4.2. Total Peat Volume Loss and Current Environmental Factors

Fire-related peat volume losses are estimated by multiplying area burned by average depth of burn, while assuming a combustion factor of one [24]. Here, peat volume losses for individual locations are calculated directly using in situ measurements at the times of the fires. The burned area was visually verified and quantified by a hand-held GPS survey, with multiple burn depth measurements, incorporating zero-values where surface fires occurred but did not burn into the peat. These methods provide accurate peat volume consumption measurements, enabling calculation of volumetric combustion factors and quantification of how they varied as the dry season progressed.

Where peat volume loss matrices were established, consumption amounts varied widely, from  $50$  to  $804 \text{ m}^3 \text{ ha}^{-1}$ . Variability was not random, however, with greater consumption rates and lower variance as the dry season progressed. Average August peat volume losses were  $102 \pm 74 \text{ m}^3 \text{ ha}^{-1}$  but grew to  $774 \pm 50 \text{ m}^3 \text{ ha}^{-1}$  in September, when lower water tables and peat moisture contents prevailed [50].



#### 4.3. Differing Peat Depth Methodology and Results

Two methodologies were developed for quantifying peat fire behaviour—(1) rate of peat fire spread (horizontal and vertical) and (2) volume loss of peat through burning. Both methodologies record depth of peat burn but findings from each are markedly different. Observed average depths at which peat fires self-extinguished, measured using the metal rods, were  $21.3 \pm 8.2$  cm in August and  $21.0 \pm 3.9$  cm in September, whereas peat burn depths measured using the matrices ranged from 0 to 30 cm and averaged 6.3 cm if limited to grid cells where peat actually burned, or 5.0 cm if all grid cells were included. We believe the primary reason for the widely differing peat burn depth measurements between methods was due to the position selection process for the iron rods versus the matrices. Rods were installed directly in front of actively burning peat sections that were entirely ignited. Matrices, in contrast, were installed up to several meters ahead of peat fires where they were considered likely to spread, but not necessarily under the same environmental conditions (e.g., wind, temperature, peat moisture content) as the rod locations experienced. Consequently, although the collected rod data recorded ranges of rates of spread within the peat, this methodology is likely to be biased towards upper limits of peat fire burning behaviour, in terms of vertical and horizontal spread. Conversely, the matrices method is likely to present a more accurate picture of the meandering, often self-extinguishing, nature of peat fires within degraded peat, often subjected to many previous fires. We also investigated if the metal rods acted as conductors of heat resulting in additional peat burning in their vicinity, however a t-test analysis between peat burn depths recorded at grid network corners, versus those not touching a rod, yielded no significant difference.

#### 4.4. Carbon Emission Calculations Sensitivity to Parametrization Factors

The above findings highlight how environmental conditions and methodology can impact parameters (e.g., average peat depth) used to calculate carbon emissions estimates. Here, we discuss each parameter used in the peat fire emissions calculation formula, and consider the accuracy, limitations and assumptions of our data, and that used in other papers published on this topic.

##### 4.4.1. Total Area of Peat Burned

Determining area burned across whole peat domes and/or landscapes requires use of remote sensing estimation techniques (e.g., [11,25,26,45]). However, substantial accuracy limitations remain for remotely assessing area burned in peatlands [28,51], and even more for the area encompassed by surface burning that experienced actual peat fires.

To make direct comparisons between studies, years, or regions, total emissions per fixed area (e.g., hectare) is often used. The methodology used in this study is limited by scale, being focused on direct measurement of area burned by individual wildfires. Few fires can be monitored in a single fire season, covering a very small fraction of total area burned. However, this provides detailed and much needed Tier 3 field data regarding micro-scale area burned [24,32], enabling extrapolation that is more accurate than simply assuming the entire peat surface burned to a fixed depth within satellite-detected burn perimeters.

##### 4.4.2. Depth of Burn

Peat burn depth is key for calculating emissions and is potentially the most variable and hardest parameter to evaluate over large areas. Our field data highlight how spatially variable measurements of peat burn depth can be, as well as how average depths of peat burning increase over time during the dry season. In addition to peat biophysical and chemical properties, such as bulk density (see below), environmental factors such as weather, peat moisture content, water table depth, distance from a water source, surface fuels, mineral content and number of times burned will all impact the depth to which peat burns [32,37,38,52,53]. Konecny et al. (2016) [25] tease apart some of these factors, specifically, how distance from canal (impacting WTD and MC%) and fire burn history

relate to burn depth. Here, we have shown how method selection for peat burn depth estimation may yield differently weighted results.

Our results obtained through the rods methods gave an average burn depth of 21–21.3 cm for August to September in areas that were intensely burning, which is close to the 23 cm reported by Simpson et al. (2016) [26] at a first-time burned site in 2015 in Jambi, using structure-from-motion photogrammetry. Similarly, Ballhorn et al. (2009) [11] reported 33 cm depths for a 2006 fire in Central Kalimantan using LiDAR that they cross-checked with ground data using the rod method. Conversely, the matrices-derived observations, with an average burn depth of 5 cm, is more like the 4 cm Konecny et al. (2016) observed using LiDAR in degraded peat locations that had burned more than three times (similar to all our FSE locations). However, the methodology Konecny et al. (2016) used did not allow for analysis of peat burns <200 m from canals—the areas most frequently and severely burnt [8,45], where we collected most of our data. This highlights the complementarity of combining multiple methods and data sources to assign appropriate burn depths to corresponding landscape locations, accounting for both proximity to canals and burn history.

#### 4.4.3. Bulk Density

The role of peat bulk density (expressed in  $\text{t ha}^{-1}$ , i.e., the mass of dry organic soil fuel) in peat-fire behaviour is unclear in the literature [53,54], but remains a major component of all peat-fire emissions estimates [24].

Peat bulk density changes consistently at different depths throughout its profile. However, near-surface (<75 cm) values differ significantly (~40%) between intact and degraded sites and with distance from canal [43]. Once the original vegetation and hydrology are removed, exposed and drained near-surface peats begin to oxidise, either through combustion or decomposition. The peat is altered or lost as a result of different degradation histories, how long the peat surface has been exposed, and the depth to which it is drained. Varying degrees of compaction and consolidation of the peat also occur as forest loss and drainage impact the peat structure, with greatest changes near canals [49]. Use of more spatially detailed and representative bulk density data would substantially improve accuracy of calculated peat fire emissions.

Bulk density analysis for the study area [42] yields  $0.1428 \text{ g cm}^{-3}$  for all FSE locations. Others have calculated bulk density directly for specific areas of study ( $0.115 \text{ g cm}^{-3}$  [25]), used a published regional bulk density (Indonesia,  $0.106 \text{ g cm}^{-3}$  [26]) or applied an approximate, appropriate value ( $0.1 \text{ g cm}^{-3}$  [11]). These different values for bulk density would result in considerable differences (20–30%) for calculated carbon emissions.

#### 4.4.4. Combustion Factor

The combustion factor is defined as the percentage of fuel available to burn that actually burned. In most studies, this value is assumed to be one, i.e., it is assumed for the given area and burn depth, all fuels burn completely. This is unlikely to be the case given the meandering and heterogeneous nature of fires burning in degraded peat. Observed peat fires regularly self-extinguished within a few days, with other locations re-igniting as additional surface fires burned across new areas. Once ignited, burn depths varied between 1 and 30 cm but these were interspersed with sections that did not burn into the peat. Assigning an accurate average depth of burn for a large heterogeneous region burning over several months would be problematic, although this issue could have been taken into account in studies using comparisons of before- and after-fire high resolution LiDAR imagery, capable of distinguishing non-burning of the peat (i.e., 0 cm burn depth) and measuring the entire surface of varied burn depths; however, this rarely is feasible (although, see Simpson et al. 2016). Factors likely influencing this behaviour include peat physical characteristics, fuel load, moisture content, depth to water table, varying weather conditions (e.g., wind, temperature, precipitation) and berm presence adjacent to canals. For observed fires, the combustion factor averaged 43% in August but grew to 88% in

September, indicating that far less peat actually burns when higher water table depths better maintain greater fuel moisture levels earlier in the dry season.

#### 4.4.5. Emission Factors

Emissions factors are defined as the mass of each gas produced from burning a kilogram of peat. The relevance, importance and variability of emissions factors is discussed in detail in Stockwell et al. (2016) [15], who derived detailed emissions factors for ~80 gases from in situ fires near the study area. Similar to bulk density, various studies have used different available emissions factor data sources in their total emissions calculations. References [15,33,55] all show that standardised factors used, for example, from IPCC or INCAS (Indonesian National Carbon Accounting System), may differ substantially between regions and under different environmental conditions. Consequently, collection of additional field data, which is spatially and temporally specific, will increase understanding of variability within and between sites and yield more accurate application of emissions factors.

#### 4.4.6. Total Emissions

We provide calculated total emissions estimates and comparisons based on common assumptions. Results are presented as biomass tonnes per hectare and tonnes carbon per hectare (Table 4).

Based on our observations, total carbon emissions were  $8.1 \pm 7.8 \text{ tC ha}^{-1}$  and  $60.2 \text{ tC ha}^{-1} \pm 13.7 \text{ tC ha}^{-1}$  in August and September, respectively. Previous studies have observed the following carbon emissions:  $134 \text{ tC ha}^{-1}$  for a combined mixture of burned and unburned sites [26];  $29.7 \text{ tC ha}^{-1}$  at an unburned site [11],  $13 \text{ tC ha}^{-1}$  (for three previous burns) to  $114 \text{ tC ha}^{-1}$  (for no previous burns) [25]; and  $27.6\text{--}124.1 \text{ tC ha}^{-1}$ —for two and no previous burns, respectively [27]. All our FSE locations had burned 3–8 times and have a comparable total carbon emission range to other study sites with similar conditions, such as the  $13 \text{ tC ha}^{-1}$  for three previous burns [25], and the  $27.6 \text{ tC ha}^{-1}$  for two previous burns [27]. All our observed fires were on sites within 200 m of canals that had burned over four times. Our late dry season (September) estimates are somewhat higher than reported emissions for sites burned multiple times [25,27]; we discuss the factors below that influence this.

Methodological choice to measure peat burn depth and related combustion factors, as well as having site-specific bulk density and emission factor data can all substantially affect total emissions estimates. We presented here our more exacting matrix method for measuring different parameters to estimate carbon emissions and determine peat volume loss, and showed how this improves upon simply using observed average burn depth with rods (here, observed with an average of  $21.3 \pm 8.2$  and  $21.3 \pm 3.9 \text{ cm}$ , for August and September, respectively). We also showed the importance of applying a corrected combustion factor (43% and 88%, respectively, for August and September) based on actual area (or in our case, volume) burned. All of our fire locations were in heavily degraded areas with higher bulk density ( $0.1428 \text{ g cm}^{-3}$  [42]) than that attained from regional level studies ( $0.106 \text{ g cm}^{-3}$ —field data throughout Indonesia [26]). Our estimated emissions values were further slightly lowered by using emissions factors from peat fires in this region in 2015 [15], during the year that we collected our data, instead of applying higher generalised values used by the IPCC (2013) [24]. Using the peat burn depth from the rod method, assumed bulk density from regional level data, a combustion factor which does not correct for percentage burn, and regional level emissions factor data as substitutes for the corresponding in situ data we have collected, would yield emissions estimate changes ranging from +798% to −26% in magnitude, depending on month and which assumptions are applied (Table 4). If we combine all the assumptions, this can lead to a +1509% increase over our actual emission calculations. The most extreme emissions overestimates happen early in the dry season when total combustion is considerably lower than the assumed 100%.

**Table 4.** The percentage change to total emissions and total C emissions calculated in this study, when using peat burn depth based on the rod methodology, regional level bulk density and emission factor data and combustion factors which do not correct for unburned area/volume (assumption values indicated in bold italics).

| Applied Assumption Variable                                       | Total Emissions    |                      | Volume                          | Bulk Density       | Combustion Factor | Emission Factor    | Carbon Emission Factor | Total Emissions  |                      |
|---|--------------------|----------------------|---------------------------------|--------------------|-------------------|--------------------|------------------------|--|----------------------|
|   | t ha <sup>−1</sup> | C-t ha <sup>−1</sup> | m <sup>3</sup> ha <sup>−1</sup> | g cm <sup>−3</sup> | Dimensionless     | g kg <sup>−1</sup> | gC kg <sup>−1</sup>    | t ha <sup>−1</sup>   | C-t ha <sup>−1</sup> |
| This study—August 2015  | 27.2               | 8.1                  | 237                             | 0.1428             | 0.43              | 1864.51            | 558.73                 | <i>effect of assumption variable—percent change to this study's data</i> |                      |
| This study—September 2015   | 200.7              | 60.2                 | 852                             | 0.1428             | 0.88              | 1864.51            | 558.73                 |  |                      |
| <i>This study—Aug—burn depth: rods method</i>                     | 243.8              | 73.0                 | <b>2130</b>                     | 0.1428             | 0.43              | 1864.51            | 558.73                 | <b>798%</b>  | <b>798%</b>          |
| <i>This study—Sept—burn depth: rods method</i>                    | 494.7              | 148.3                | <b>2100</b>                     | 0.1428             | 0.88              | 1864.51            | 558.73                 | <b>146%</b>  | <b>146%</b>          |
| <i>This study—Aug—country-scale Indonesian bulk density data</i>  | 20.1               | 6.0                  | 237                             | <b>0.106</b>       | 0.43              | 1864.51            | 558.73                 | <b>−26%</b>  | <b>−26%</b>          |
| <i>This study—Sept—country-scale Indonesian bulk density data</i> | 149.0              | 44.7                 | 852                             | <b>0.106</b>       | 0.88              | 1864.51            | 558.73                 | <b>−26%</b>  | <b>−26%</b>          |
| <i>This study—Aug—Combustion factor of one</i>                    | 63.2               | 18.9                 | 237                             | 0.1428             | <b>1</b>          | 1864.51            | 558.73                 | <b>133%</b>  | <b>133%</b>          |
| <i>This study—Sept—Combustion factor of one</i>                   | 226.9              | 68.0                 | 852                             | 0.1428             | <b>1</b>          | 1864.51            | 558.73                 | <b>13%</b>   | <b>13%</b>           |
| <i>This study—Aug—IPCC EFs</i>                                    | 28.2               | 8.3                  | 237                             | 0.1428             | 0.43              | <b>1934.10</b>     | <b>570.70</b>          | <b>4%</b>  | <b>2%</b>            |
| <i>This study—Sep—IPCC EFs</i>                                    | 208.2              | 61.4                 | 852                             | 0.1428             | 0.88              | <b>1934.10</b>     | <b>570.70</b>          | <b>4%</b>  | <b>2%</b>            |
| <i>This study plus all general assumptions—Aug</i>                | <b>436.7</b>       | <b>128.9</b>         | <b>2130</b>                     | <b>0.106</b>       | <b>1</b>          | <b>1934.10</b>     | <b>570.70</b>          | <b>1509%</b>   | <b>1484%</b>         |
| <i>This study plus all general assumptions—Sep</i>                | <b>430.5</b>       | <b>127.0</b>         | <b>2100</b>                     | <b>0.106</b>       | <b>1</b>          | <b>1934.10</b>     | <b>570.70</b>          | <b>114%</b>  | <b>111%</b>          |



It is important to note that, as the dry season progresses in severity, peat dome water tables drop, increasing surface dryness and surface fuel availability [50]. This substantially affects total emissions as vertical and horizontal peat-fire spread rates, peat volumes burned, and combustion factors are all exacerbated as the peat dries. Our data were collected during 2015, one of the driest years on record. Wetter years will result in peat fire behaviour and associated emissions that may be more in line with our August estimates.

It should also be noted that collection of peat fire data was only possible at six locations during the 2015 dry season due to challenges accessing fire locations when low water levels hampered travel along many canals and fire risks made staying out on the peat without any safe manner of egress untenable. Therefore, statistical analyses correlating prevailing environmental conditions with observed peat fire behaviour (as might be conducted under controlled laboratory conditions) were precluded. Water table depth, moisture content, fire history, temperature and wind speed, all recorded in this study (Supplementary Material S2), have been shown to influence fire behaviour [34–37]. The variability observed in both the environmental and peat fire data collected highlights the range of field conditions but this variability illustrates the need for large sample sizes to statistically separate out cause and effect. It is noted, given the challenges facing in situ data collection at a meaningful scale for burning peat fires, this approach could be combined with eddy-covariance flux tower data, where available, as a means to verify and scale up FSE data collection from a micro- to a landscape scale.

## 5. Conclusions

This is the first study to have collected all data for peat-fire emission calculations directly from the affected peatlands. This methodology is both enhanced and limited by its micro-scale nature. It provides a degree of accuracy and detail that is much needed to support, verify and calibrate remotely sensed data. However, in and of itself, it cannot be scaled to provide emissions estimates for regional landscapes. The results from this study illustrate the importance of accounting for such factors as (1) methodological choice and how this might impact overall emissions; (2) temporal effect of drought intensity, which reduces water table depths and fuel moisture values, yielding faster fire spread rates and greater fuel consumption; (3) disturbance history, that results in greater bulk density, and hence increases emissions per unit of combusted peat volume; and (4) improved emissions factors, which may be region-specific. This information can be used to enhance the accuracy of model and remote sensing-based emissions estimates from burning in tropical peatlands.

**Supplementary Materials:** The following supporting information can be downloaded at: <https://www.mdpi.com/article/10.3390/fire5030062/s1>: Supplementary Material S1: FSE field sketches and photos; Supplementary Material S2: Raw data including environmental data.

**Author Contributions:** Conceptualization, L.L.B.G. and G.B.A.; Data curation, L.L.B.G. and A.T.; Formal analysis, L.L.B.G.; Investigation, L.L.B.G., G.B.A. and A.T.; Methodology, L.L.B.G., G.B.A., A.T., K.C.R. and M.A.C.; Writing—original draft, L.L.B.G.; Writing—review and editing, G.B.A., B.H.S. and M.A.C. All authors have read and agreed to the published version of the manuscript.

**Funding:** The data research was funded by NASA grants (NNX13AP46G, NNX17AC95G, 80NSSC18K0235). We also acknowledge the ACIAR FST 2016-144 project which also supports and implements these FSE methods.

**Institutional Review Board Statement:** Not applicable.

**Informed Consent Statement:** Not applicable.

**Data Availability Statement:** The data presented in this study are available either within this article or can be found within the Supplementary Material.

**Acknowledgments:** Thanks go to the Borneo Orangutan Foundation Mawas-Program Environmental Monitoring and Research Field team—Ahmad Yunan, Ramadhan, Ato, Didie and Agus.

**Conflicts of Interest:** The authors declare no conflict of interest. The funders had no role in the design of the study, in the collection, analyses, or interpretation of data, in the writing of the manuscript, or in the decision to publish the results.

## References

- Page, S.E.; Rieley, J.O.; Banks, C.J. Global and Regional Importance of the Tropical Peatlands Carbon Pool. *Glob. Chang. Biol.* **2011**, *17*, 798–818. [\[CrossRef\]](#)
- Page, S.E.; Rieley, J.O.; Shotyk, Ø.W.; Weiss, D. Interdependence of Peat and Vegetation in a Tropical Peat Swamp Forest. *Philos. Trans. R. Soc. Lond. B* **1999**, *354*, 1885–1897. [\[CrossRef\]](#) [\[PubMed\]](#)
- Dommain, R.; Couwenberg, J.; Joosten, H. Hydrological Regulation of Domed Peatlands in South-East Asia and Consequences for Conservation and Restoration. *Mires Peat* **2010**, *6*, 1–17.
- Turetsky, M.R.; Benscoter, B.; Page, S.; Rein, G.; van der Werf, G.R.; Watts, A. Global Vulnerability of Peatlands to Fire and Carbon Loss. *Nat. Geosci.* **2015**, *8*, 11–14. [\[CrossRef\]](#)
- Harrison, M.E.; Ottay, J.B.; D’Arcy, L.J.; Cheyne, S.M.; Anggodo; Belcher, C.; Cole, L.; Dohong, A.; Ermiasi, Y.; Feldpausch, T.; et al. Tropical Forest and Peatland Conservation in Indonesia: Challenges and Directions. *People Nat.* **2020**, *2*, 4–28. [\[CrossRef\]](#)
- Langner, A.; Miettinen, J.; Siegert, F. Land Cover Change 2002–2005 in Borneo and the Role of Fire Derived from MODIS Imagery. *Glob. Chang. Biol.* **2007**, *13*, 2329–2340. [\[CrossRef\]](#)
- Dohong, A.; Aziz, A.A.; Dargusch, P. A Review of the Drivers of Tropical Peatland Degradation in South-East Asia. *Land Use Policy* **2017**, *69*, 349–360. [\[CrossRef\]](#)
- Medrilzam, M.; Smith, C.; Aziz, A.A.; Herbohn, J.; Dargusch, P. Smallholder Farmers and the Dynamics of Degradation of Peatland Ecosystems in Central Kalimantan, Indonesia. *Ecol. Econ.* **2017**, *136*, 101–113. [\[CrossRef\]](#)
- Miettinen, J.; Liew, S.C. Degradation and Development of Peatlands in Peninsular Malaysia and in the Islands of Sumatra and Borneo since 1990. *Land Degrad. Dev.* **2010**, *21*, 285–296. [\[CrossRef\]](#)
- Page, S.E.; Siegert, F.; Rieley, J.O.; Boehm, H.-D.D.V.; Jaya, A.; Limin, S. The Amount of Carbon Released from Peat and Forest Fires in Indonesia in 1997. *Nature* **2002**, *420*, 61–65. [\[CrossRef\]](#)
- Ballhorn, U.; Siegert, F.; Mason, M.; Limin, S.; Limin, S. Derivation of Burn Scar Depths and Estimation of Carbon Emissions with LIDAR in Indonesian Peatlands. *Proc. Natl. Acad. Sci. USA* **2009**, *106*, 21213–21218. [\[CrossRef\]](#) [\[PubMed\]](#)
- Van Der Werf, G.R.; Randerson, J.T.; Giglio, L.; Collatz, G.J.; Mu, M.; Kasibhatla, P.S.; Morton, D.C.; Defries, R.S.; Jin, Y.; Van Leeuwen, T.T. Global Fire Emissions and the Contribution of Deforestation, Savanna, Forest, Agricultural, and Peat Fires (1997–2009). *Atmos. Chem. Phys.* **2010**, *10*, 11707–11735. [\[CrossRef\]](#)
- Miettinen, J.; Shi, C.; Liew, S.C. Fire Distribution in Peninsular Malaysia, Sumatra and Borneo in 2015 with Special Emphasis on Peatland Fires. *Environ. Manag.* **2017**, *60*, 747–757. [\[CrossRef\]](#)
- Jayarathne, T.; Stockwell, C.E.; Gilbert, A.A.; Daugherty, K.; Cochrane, M.A.; Ryan, K.C.; Putra, E.I.; Saharjo, B.H.; Nurhayati, A.D.; Albar, I.; et al. Chemical Characterization of Fine Particulate Matter Emitted by Peat Fires in Central Kalimantan, Indonesia, during the 2015 El Niño. *Atmos. Chem. Phys.* **2018**, *18*, 2585–2600. [\[CrossRef\]](#)
- Stockwell, C.E.; Jayarathne, T.; Cochrane, M.A.; Ryan, K.C.; Putra, E.I.; Saharjo, B.H.; Nurhayati, A.D.; Albar, I.; Blake, D.R.; Simpson, I.J.; et al. Field Measurements of Trace Gases and Aerosols Emitted by Peat Fires in Central Kalimantan, Indonesia, during the 2015 El Niño. *Atmos. Chem. Phys.* **2016**, *16*, 11711–11732. [\[CrossRef\]](#)
- BMKG. Badan Meteorologi, Klimatologi dan Geofisika—Kualitas Udara—Informasi Konsentrasi Partikulat (PM10). Available online: <http://www.bmkg.go.id/kualitas-udara/informasi-partikulat-pm10.bmkg> (accessed on 20 October 2015).
- Johnston, F.H.; Melody, S.; Bowman, D.M.J.S. The Pyrohealth Transition: How Combustion Emissions Have Shaped Health through Human History. *Philos. Trans. R. Soc. B Biol. Sci.* **2016**, *371*, 20150173. [\[CrossRef\]](#)
- Kopplitz, S.N.; Mickley, L.J.; Marlier, M.E.; Buonocore, J.J.; Kim, P.S.; Liu, T.; Sulprizio, M.P.; DeFries, R.S.; Jacob, D.J.; Schwartz, J.; et al. Public Health Impacts of the Severe Haze in Equatorial Asia in September–October 2015: Demonstration of a New Framework for Informing Fire Management Strategies to Reduce Downwind Smoke Exposure. *Environ. Res. Lett.* **2016**, *11*, 094023. [\[CrossRef\]](#)
- Kok, L.M. Haze in Singapore: A Problem Dating Back 40 Years. Available online: <https://www.straitstimes.com/singapore/environment/haze-in-singapore-a-problem-dating-back-40-years> (accessed on 14 February 2019).
- Goldstein, J.E. Lots of Smoke, but Where’s the Fire? Contested Causality and Shifting Blame in Southeast Asia’s Smoke-Haze Crisis. In *The Quotidian Anthropocene: Reconfiguring Environments in Urbanizing Asia*; Vaughn, E.T., Elinoff, K.F., Eds.; University of Pennsylvania Press: Philadelphia, PA, USA, 2017. [\[CrossRef\]](#)
- Huijnen, V.; Wooster, M.J.; Kaiser, J.W.; Gaveau, D.L.A.; Flemming, J.; Parrington, M.; Inness, A.; Murdiyarso, D.; Main, B.; van Weele, M. Fire Carbon Emissions over Maritime Southeast Asia in 2015 Largest since 1997. *Sci. Rep.* **2016**, *6*, 26886. [\[CrossRef\]](#)
- van der Werf, G.R.; Morton, D.C.; DeFries, R.S.; Olivier, J.G.J.; Kasibhatla, P.S.; Jackson, R.B.; Collatz, G.J.; Randerson, J.T. CO<sub>2</sub> Emissions from Forest Loss. *Nat. Geosci.* **2009**, *2*, 737–738. [\[CrossRef\]](#)
- Hu, Y.; Fernandez-Anez, N.; Smith, T.E.L.; Rein, G. Review of Emissions from Smouldering Peat Fires and Their Contribution to Regional Haze Episodes. *Int. J. Wildl. Fire* **2018**, *27*, 293–312. [\[CrossRef\]](#)

24. Drosler, M.; Verchott, L.V.; Freibauer, A. Chapter 2: Drained Inland Organic Soils. In *2013 Supplement to the 2006 IPCC Guidelines for National Greenhouse Gas Inventories: Wetlands*; Hiraiishi, T., Krug, T., Tanabe, K., Srivastava, N., Jamsranjav, B., Fukuda, M., Troxler, T., Eds.; IPCC: Geneva, Switzerland, 2014; pp. 2.1–2.74.
25. Konecny, K.; Ballhorn, U.; Navratil, P.; Jubanski, J.; Page, S.E.; Tansey, K.; Hooijer, A.; Vernimmen, R.; Siegert, F. Variable Carbon Losses from Recurrent Fires in Drained Tropical Peatlands. *Glob. Chang. Biol.* **2016**, *22*, 1469–1480. [\[CrossRef\]](#) [\[PubMed\]](#)
26. Simpson, J.E.; Wooster, M.J.; Smith, T.E.L.; Trivedi, M.; Vernimmen, R.R.E.; Dedi, R.; Shakti, M.; Dinata, Y. Tropical Peatland Burn Depth and Combustion Heterogeneity Assessed Using Uav Photogrammetry and Airborne LiDAR. *Remote Sens.* **2016**, *8*, 1000. [\[CrossRef\]](#)
27. Krisnawati, H.; Imanuddin, R.; Adinugroho, W.C.; Hutabarat, S. Chapter 7: Standard Method—Peatland GHG Emissions. In *Standard Methods for Estimating Greenhouse Gas Emissions from Forests and Peatlands in Indonesia (Version 2)*; Research, Development and Innovation Agency of the Ministry of Environment and Forestry: Bogor, Indonesia, 2015; pp. 44–51.
28. Tansey, K.; Beston, J.; Hoscilo, A.; Page, S.E.; Paredes, H.C.U. Relationship between MODIS Fire Hot Spot Count and Burned Area in a Degraded Tropical Peat Swamp Forest in Central Kalimantan, Indonesia. *J. Geophys. Res. D Atmos.* **2008**, *113*. [\[CrossRef\]](#)
29. Cheng, D.; Rogan, J.; Schneider, L.; Cochrane, M. Evaluating MODIS Active Fire Products in Subtropical Yucatán Forest. *Remote Sens. Lett.* **2013**, *4*, 455–464. [\[CrossRef\]](#)
30. Toomey, M.; Roberts, D.A.; Caviglia-Harris, J.; Cochrane, M.A.; Dewes, C.F.; Harris, D.; Numata, I.; Sales, M.H.; Sills, E.; Souza, C.M., Jr. Long-Term, High-Spatial Resolution Carbon Balance Monitoring of the Amazonian Frontier: Predisturbance and Postdisturbance Carbon Emissions and Uptake. *J. Geophys. Res. Biogeosciences* **2013**, *118*, 400–411. [\[CrossRef\]](#)
31. Jessup, T.C.; Vayda, A.P.; Cochrane, M.A.; Applegate, G.B.; Ryan, K.C.; Saharjo, B.H. Why Estimates of the Peat Burned in Fires in Sumatra and Kalimantan Are Unreliable and Why It Matters. *Singap. J. Trop. Geogr.* **2022**, *43*, 7–25. [\[CrossRef\]](#)
32. Watts, A.C. Organic Soil Combustion in Cypress Swamps: Moisture Effects and Landscape Implications for Carbon Release. *For. Ecol. Manag.* **2013**, *294*, 178–187. [\[CrossRef\]](#)
33. Smith, T.E.L.; Evers, S.; Yule, C.M.; Gan, J.Y. In Situ Tropical Peatland Fire Emission Factors and Their Variability, as Determined by Field Measurements in Peninsula Malaysia. *Glob. Biogeochem. Cycles* **2018**, *32*, 18–31. [\[CrossRef\]](#)
34. Prat-Guitart, N.; Rein, G.; Hadden, R.M.; Belcher, C.M.; Yearsley, J.M. Propagation Probability and Spread Rates of Self-Sustained Smouldering Fires under Controlled Moisture Content and Bulk Density Conditions. *Int. J. Wildl. Fire* **2016**, *25*, 456. [\[CrossRef\]](#)
35. Prat-Guitart, N.; Rein, G.; Hadden, R.M.; Belcher, C.M.; Yearsley, J.M. Effects of Spatial Heterogeneity in Moisture Content on the Horizontal Spread of Peat Fires. *Sci. Total Environ.* **2016**, *572*, 1422–1430. [\[CrossRef\]](#)
36. Huang, X.; Rein, G. Upward-and-Downward Spread of Smoldering Peat Fire. *Proc. Combust. Inst.* **2018**, *37*, 4025–4033. [\[CrossRef\]](#)
37. Huang, X.; Restuccia, F.; Gramola, M.; Rein, G. Experimental Study of the Formation and Collapse of an Overhang in the Lateral Spread of Smoldering Peat Fires. *Combust. Flame* **2016**, *168*, 393–402. [\[CrossRef\]](#)
38. Rein, G. *Fire Phenomena in the Earth System: An Interdisciplinary Approach to Fire Science*; Belcher, C., Ed.; John Wiley & Sons Ltd.: Hoboken, NJ, USA, 2013. [\[CrossRef\]](#)
39. Rollins, M.S.; Cohen, A.D.; Durig, J.R. Effects of Fires on the Chemical and Petrographic Composition of Peat in the Snuggedy Swamp, South Carolina. *Int. J. Coal Geol.* **1993**, *22*, 101–117. [\[CrossRef\]](#)
40. Turetsky, M.R.; Donahue, W.F.; Benscoter, B.W. Experimental Drying Intensifies Burning and Carbon Losses in a Northern Peatland. *Nat. Commun.* **2011**, *2*, 514. [\[CrossRef\]](#)
41. Applegate, G.; Graham, L.L.B.; Thomas, A.; Yunan, A.; Didie, Agus; Ato; Saharjo, B.H.; Cochrane, M. *Fire Scene Evaluation Field Manual*; IPB Press: Bogor, Indonesia, 2018.
42. Sinclair, A.L.; Graham, L.L.B.; Putra, E.I.; Saharjo, B.H.; Applegate, G.; Grover, S.P.; Cochrane, M.A. Effects of Distance from Canal and Degradation History on Peat Bulk Density in a Degraded Tropical Peatland. *Sci. Total Environ.* **2020**, *699*, 134199. [\[CrossRef\]](#)
43. Wedeux, B.; Dalponte, M.; Schlund, M.; Hagen, S.; Cochrane, M.; Graham, L.; Usup, A.; Thomas, A.; Coomes, D. Dynamics of a Human-Modified Tropical Peat Swamp Forest Revealed by Repeat Lidar Surveys. *Glob. Chang. Biol.* **2020**, *26*, 3947–3964. [\[CrossRef\]](#)
44. Dephut. Rencana Induk (Master Plan) Rehabilitasi dan Konservasi Kawasan Pengembangan Lahan Gambut di Propinsi Kalimantan Tengah. In *Pusat Rencana dan Statistik Kehutanan*; Kehutanan, B.P., Ed.; Badan Planologi Kehutanan: Jakarta, Indonesia, 2007.
45. Vetrita, Y.; Cochrane, M.A. *Annual Burned Area from Landsat, Mawas, Central Kalimantan, Indonesia, 1997–2015*; ORNL DAAC: Oak Ridge, TN, USA, 2019. [\[CrossRef\]](#)
46. Goldstein, J.E.; Graham, L.; Ansori, S.; Vetrita, Y.; Thomas, A.; Applegate, G.; Vayda, A.P.; Saharjo, B.H.; Cochrane, M.A. Beyond Slash-and-Burn: The Roles of Human Activities, Altered Hydrology and Fuels in Peat Fires in Central Kalimantan, Indonesia. *Singap. J. Trop. Geogr.* **2020**, *41*, 190–208. [\[CrossRef\]](#)
47. Phillips, T. The Mathematics of Surveying. Available online: <http://www.ams.org/samplings/feature-column/fcarc-surveying-one> (accessed on 2 May 2018).
48. Ichsan, N.; Hooijer, A.; Vernimmen, R.; Applegate, G.B. KFCP Hydrology and Peat Monitoring Methodology; Scientific Report. 2014. Available online: [http://simlit.puspijak.org/files/buku/KFCP\\_Hydrology\\_and\\_Peat\\_Monitoring\\_Methodology\\_S1.pdf](http://simlit.puspijak.org/files/buku/KFCP_Hydrology_and_Peat_Monitoring_Methodology_S1.pdf) (accessed on 15 October 2021).
49. Hooijer, A.; Page, S.E.; Jauhainen, J.; Lee, W.A.; Lu, X.X.; Idris, A.; Anshari, G. Subsidence and Carbon Loss in Drained Tropical Peatlands. *Biogeosciences* **2012**, *9*, 1053–1071. [\[CrossRef\]](#)

- 
50. Putra, E.I.; Cochrane, M.A.; Vetrina, Y.; Graham, L.; Saharjo, B.H. Determining Critical Groundwater Level to Prevent Degraded Peatland from Severe Peat Fire. *IOP Conf. Ser. Earth Environ. Sci.* **2018**, *149*, 012027. [[CrossRef](#)]
  51. Vetrina, Y.; Cochrane, M.A.; Suwarsono; Priyatna, M.; Sukowati, K.A.D.; Khomarudin, M.R. Evaluating Accuracy of Four MODIS-Derived Burned Area Products for Tropical Peatland and Non-Peatland Fires. *Environ. Res. Lett.* **2021**, *16*, 035015. [[CrossRef](#)]
  52. Huang, X.; Rein, G. Computational Study of Critical Moisture and Depth of Burn in Peat Fires. *Int. J. Wildl. Fire* **2015**, *24*, 798. [[CrossRef](#)]
  53. Benscoter, B.W.; Thompson, D.; Waddington, J.M.; Flannigan, M.; Wotton, B.M.; De Groot, W.J.; Turetsky, M.R. Interactive Effects of Vegetation, Soil Moisture and Bulk Density on Depth of Burning of Thick Organic Soils. *Int. J. Wildl. Fire* **2011**, *20*, 418–429. [[CrossRef](#)]
  54. Garlough, E.C.; Keyes, C.R. Influences of Moisture Content, Mineral Content and Bulk Density on Smouldering Combustion of Ponderosa Pine Duff Mounds. *Int. J. Wildl. Fire* **2011**, *20*, 589–596. [[CrossRef](#)]
  55. Kiely, L.; Spracklen, D.V.; Wiedinmyer, C.; Conibear, L.; Reddington, C.L.; Archer-Nicholls, S.; Lowe, D.; Arnold, S.R.; Knote, C.; Khan, M.F.; et al. New Estimate of Particulate Emissions from Indonesian Peat Fires in 2015. *Atmos. Chem. Phys.* **2019**, *19*, 11105–11121. [[CrossRef](#)]